Thermal stability and kinetic degradation study for dihydroartemisinin

Denisa Circioban[1] · Adriana Ledeti[1] · Gabriela Vlase[2] · Titus Vlase[2] · Cristina Dehelean[1] · Ionut Ledeti[1]

Abstract

Dihydroartemisinin (DHA), the hydrogenated derivative of the naturally originated sesquiterpene lactone artemisinin, is a well-known antimalarial agent that is currently researched because of its potential as an anticancer medication. Because DHA has been associated with a low oral bioavailability and a short half-life, new formulations meant to overcome these shortcomings are currently under development. As such, the present paper aims to present a comprehensive physico-chemical profile of DHA containing data of great importance for the preformulation stages of the drug design process. As instrumental techniques, attenuated total reflection Fourier transform infrared spectroscopy (ATR-FTIR) spectroscopy and thermal analysis (TG—thermogravimetric/DTG—derivative thermogravimetric/HF—heat flow) were performed, followed by a kinetic study realized using three isoconversional methods (Friedman—Fr, Flynn–Wall–Ozawa—FWO and Kissinger–Akahira–Sunose—KAS), as well as the nonparametric kinetic method (NPK). FTIR spectroscopy confirmed the identity and purity of DHA, and thermal analysis revealed a relatively low thermal stability and a multistep thermooxidation that was proved during the performed kinetic study. The latter unveiled a two-process decomposition determined by both chemical degradations and physical transformations.

Keywords Dihydroartemisinin · Thermal stability · FTIR · Kinetic study · NPK method

Abbreviations

t	Time
T	Temperature
α	Conversion degree
$f(\alpha)$	The differential conversion function
R	The universal gas constant
$g(\alpha)$	The integral conversion function
β	The heating rate
$k(T)$	The temperature dependence function
A	The pre-exponential factor
E_a	The apparent activation energy given by the Arrhenius equation

✉ Adriana Ledeti
afulias@umft.ro

1 Faculty of Pharmacy, University of Medicine and Pharmacy "Victor Babeş", Eftimie Murgu Square 2, 300041 Timişoara, Romania

2 Research Centre for Thermal Analysis in Environmental Problems, West University of Timisoara, Pestalozzi Street 16, 300115 Timişoara, Romania

Introduction

Dihydroartemisinin (DHA) or artenimol, the first semi-synthetic derivative of the naturally originated sesquiterpene lactone artemisinin (ART), was originally obtained by Professor Tu Youyou in 1973. After she managed to extract artemisinin from the aerial parts of *Artemisia annua* and prove its antimalarial effect, the Chinese Professor focused her attention towards developing compounds that would improve the solubility of the active substance, while maintaining its biological activity [1].

Along the years, numerous artemisinin-like derivatives containing the endoperoxide bridge were synthesized and analysed, research revealing they possess multiple biological applications. Among these, the initially discovered antimalarial effect and the currently researched anticancer activities make these compounds important molecules in pharmacological studies [2–4].

In order to obtain DHA, the lactone moiety of artemisinin is transformed into a lactol during a reduction reaction, in the presence of different mild hydride-reducing agents, such as sodium borohydride [5]. The process manages to preserve intact the characteristic endoperoxide moiety, a highly desired aspect, since the biological activity of these

derivatives was found to be a direct consequence of the presence of said functional group [6].

DHA (Fig. 1) is a mixture of two lactol hemiacetal epimers (α and β) that are interconverting. The hydroxyl moiety of the α-epimer was determined to be in the equatorial position, while for the β-epimer, the same group was observed to take an axial arrangement [7]. Although in solid-state DHA was found to exist solely as a β-epimer, the two epimers equilibrate during dissolution, their determined ratio varying with the used solvent. Furthermore, when found in aqueous solutions, DHA was proved to be unstable, suffering a decomposition process in both dilute acids and bases [8–10]. According to the literature, DHA presents with a melting point of approximatively 153–154 °C and a molecular mass of 284.352 g mol^{-1} and it is slightly more water-soluble than ART [9].

Despite its improved water solubility when compared to that of ART, the dissolution of DHA in water is still relatively difficult because of its three-ring organic structure [11]. This, coupled with its instability in aqueous solutions, was proved to determine a low bioavailability for DHA when administered orally ($\approx 45\%$) [12]. The 0.9–1.6 h period required until the maximal concentration is achieved after absorption and the short elimination half-time of ≈ 40 min [13] are further proof that a need has surfaced regarding the development of new formulations containing the drug that possess high solubility, increased bioavailability and controlled release [14]. A few attempts have been made in this direction, simple or magnetic liposome formulations [15, 16], nanoparticles [14, 17] or complexes with cyclodextrins and polyethylene glycol [18, 19] being synthesized and preliminary tested.

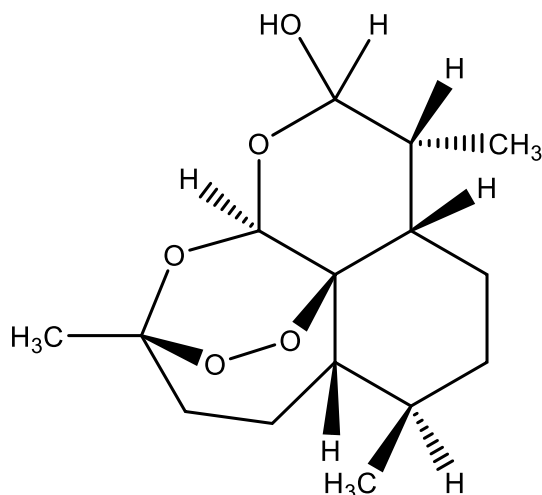Because of these aspects, the aim of the present study was represented by the determination of a comprehensive physico-chemical analysis of DHA that could provide valuable information required for the preparation of new formulations containing this pharmaceutical agent. A complete FTIR spectroscopy analysis was performed, followed by a thermal analysis (TG/DTG/HF) realized using five different heating rates that revealed the behaviour of DHA in solid state when subjected to thermal stress. The observed decomposition process was then studied from a kinetic perspective, following the ICTAC 2000 protocol and employing three isoconversional methods (the differential Friedman method and the integral Flynn–Wall–Ozawa and Kissinger–Akahira–Sunose methods), as well as the nonparametric kinetic method (NPK).

Materials and methods

Dihydroartemisinin was acquired from Sigma-Aldrich (Germany) as an analytical standard containing a mixture of both α and β isomers. The sample was stored in sealed vials protected from light, as specified by the manufacturer, and was used as received (purity $\geq 97\%$).

The attenuated total reflection Fourier transform infrared spectroscopy (ATR-FTIR) technique was applied in order to obtain the spectra of the active pharmaceutical agent. A PerkinElmer SPECTRUM 100 device was used, and the data were collected on the spectral range 4000–600 cm^{-1} after 32 consecutive determinations performed at a 4 cm^{-1} resolution. The spectral range 2750–1550 cm^{-1} was suppressed from the spectra, since no bands were observed for DHA here.

Solid samples of approximately 5 mg were weighted in open aluminium crucibles in order to carry out the thermal analysis. A PerkinElmer DIAMOND TG/DTA equipment was used, and the samples were subjected to a controlled heating protocol in a synthetic air atmosphere (flow rate equal to 100 mL min^{-1}). The thermoanalytical data (TG/DTG/HF) were collected using five different heating rates ($\beta = 5, 7, 10, 12$ and 15 °C min^{-1}) on a temperature range found between ambient conditions and 500 °C. In order to determine the thermal effects, the DTA data (in μV) were converted to HF data (in mW).

The kinetic study was performed for the main decomposition process (135–300 °C) using the previously obtained thermoanalytical data. The kinetic parameters were determined using the Friedman (Fr) isoconversional differential method [20], the Flynn–Wall–Ozawa (FWO) [21–23] and Kissinger–Akahira–Sunose (KAS) [24, 25] isoconversional integral methods and the nonparametric kinetic method (NPK), developed by Serra R., Sempere J. et al. [26–29] and later modified by Vlase T. et al. [30, 31]. The transformation range taken into account was $5\% \leq \alpha \leq 95\%$, and a variation stage for the conversion degree (α) equal to 5%

Fig. 1 The chemical structure of DHA

was used for the estimation of the apparent activation energies (E_a) values.

Results and discussion

ATR-FTIR spectroscopy

The ART-FTIR spectroscopy technique was employed as to obtain the complete FTIR spectrum of DHA. The main structural characteristics of DHA correlated with bands observed on the spectrum presented in Fig. 2 proved the identity and purity of the tested compound and showed to be in agreement with literature data [18, 32]. As the hydrogenated derivative of ATS, DHA presents a very similar spectrum to the one of its "parent" compound (previously reported by our research team [33]). Since the main structural difference separating ART from its derivative DHA is due to the reduction of the C=O bond from the saturated δ-lactone, which leads to the formation of a primary alcohol −OH group, the FTIR spectra of DHA reveal in the 3450–3300 cm^{-1} spectral range a wide band with maximum intensity reached at 3372 cm^{-1}. This is characteristic to the stretching vibration of the O–H bond, the shift from usually higher wavenumbers for this type of bond being probably a consequence of the formation of intermolecular hydrogen bonds.

The asymmetric and symmetric stretching vibration of the C–H bond from DHA's methyl and methylene moieties determines the appearance of peaks at 2945, 2926, 2924 and 2853 cm^{-1}. The band formed at 1444 cm^{-1} can be associated with the scissoring bending vibration of the C–H bond found in the cyclic −CH$_2$−groups. The symmetric bending vibration of the C–H bond from the lateral methyl groups determines the appearance of a band seen at 1377 cm^{-1},

while the wagging vibration of the methylene moiety forms a peak seen at 1227 cm^{-1}.

The bending vibration of the C–O–O–C bond corresponding to the characteristic endoperoxide bridge is revealed by bands seen at 1188 and 1176 cm^{-1}. The asymmetric stretching vibration of the C–O–C bonds is revealed by an intense peak observed at 1092 cm^{-1}, but the branching of the carbon atoms adjacent to the oxygen atom from the C–O–C group may be responsible for the splitting of said peak and the detection of additional bands at 1160 and 1135 cm^{-1}. A low intensity band noticed at 1061 cm^{-1} can be correlated with the rocking vibration of the laterally positioned methyl groups. While the stretching vibration of the C–O bond from the primary alcohol moiety can be associated with peaks revealed on the spectrum at 1023 and 1013 cm^{-1}, the vibration of the C–O–O group determines the formation of the most intense spectral band that can be observed at 984 cm^{-1}. A peak seen at 876 cm^{-1} that can be correlated with the stretching vibration of the O–O bond can also be identified. At the lower and of the spectrum, the rocking vibration of the C–H bond from the methylene group is revealed by bands seen at 755 and 732 cm^{-1}.

Thermal analysis

In order to characterize the thermal behaviour of the pharmaceutical agent, the thermal analysis was performed using multiple heating rates, a protocol established by International Confederation for Thermal Analysis and Calorimetry (ICTAC) [34] and previously employed by our research team [35–39]. The obtained thermoanalytical curves for DHA using the five selected heating rates $\beta = 5$, 7, 10, 12 and 15 °C min^{-1} are presented as superimposed mass curves (Fig. 3a), derivative mass curves (Fig. 3b) and heat flow
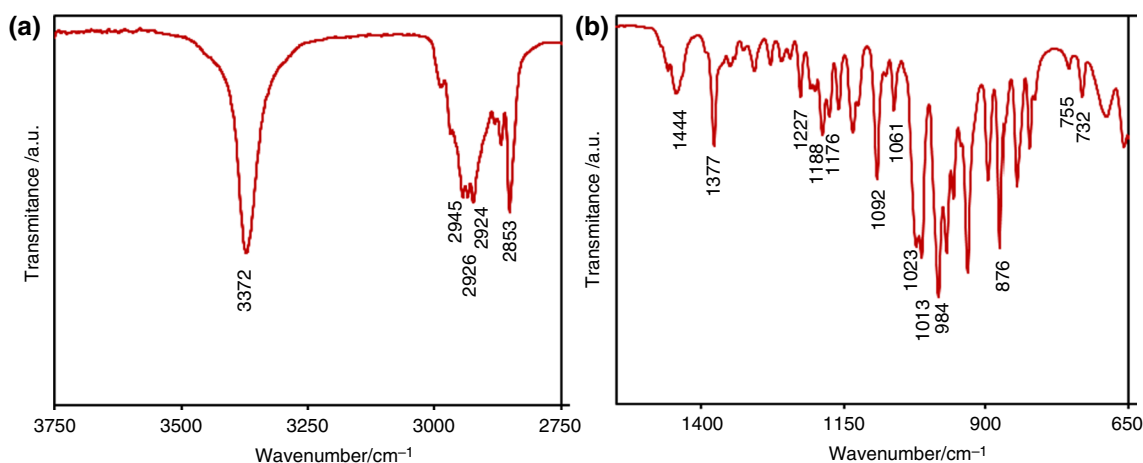
Fig. 2 The ATR-FTIR obtained spectrum for DHA: spectral range 3750–2750 cm^{-1} (**a**) and 1550–650 cm^{-1} (**b**)
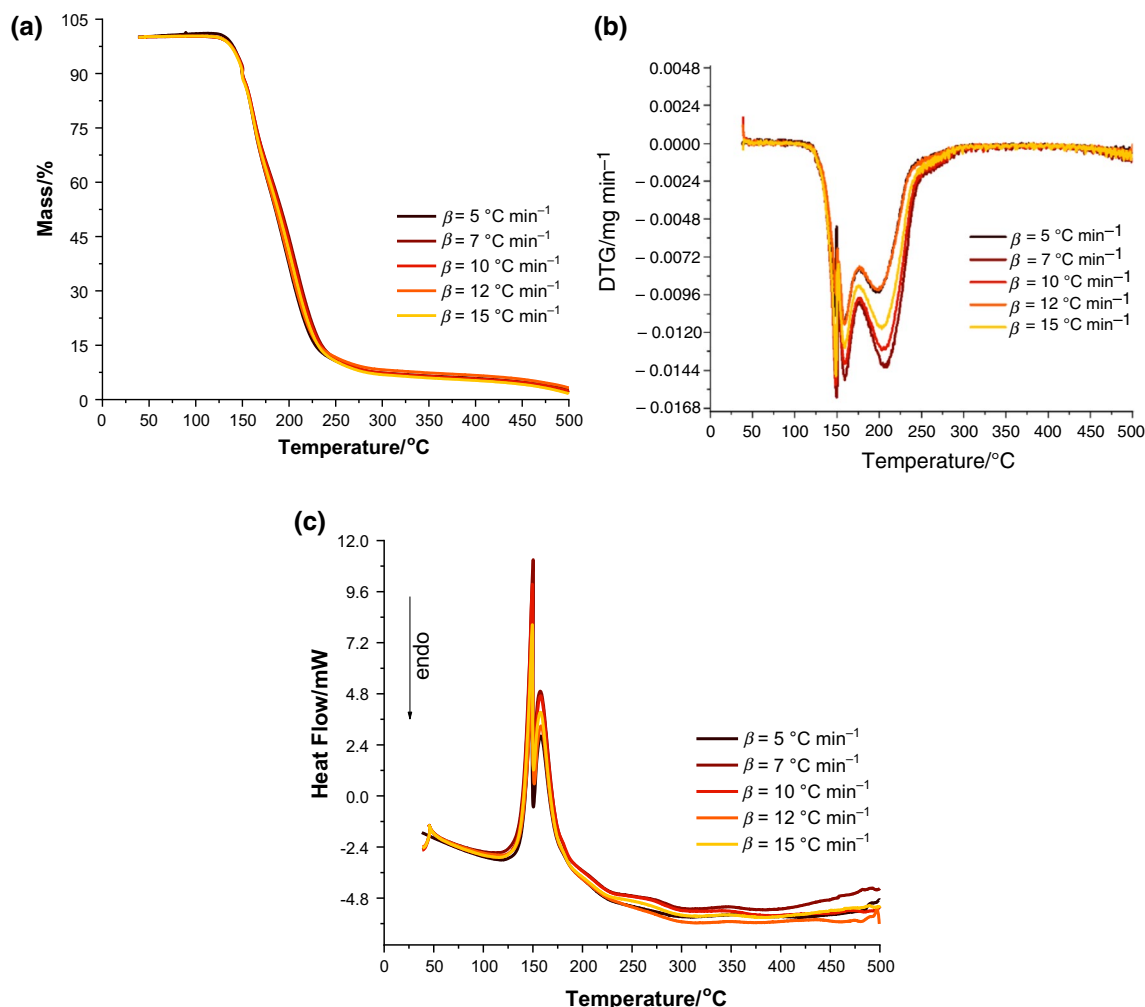
Fig. 3 Thermoanalytical superimposed curves (TG (**a**), DTG (**b**) and HF (**c**)) obtained for DHA using five different heating rates ($\beta = 5$, 7, 10, 12 and 15 °C min^{-1})

curves (Fig. 3c), while the registered data for each used heating rate are revealed in Table 1.

Studying the TG curves registered at each heating rate, a thermal stability up to 132–135 °C can be noted. A slight mass increase is more easily visible on the TG curve obtained while using a heating rate of 5 °C min^{-1} and is probably a consequence of a mild oxidation of the sesquiterpene lactol structure, by inserting this atom in the moiety

of DHA, since the thermal treatment is realized in dynamic dioxygen atmosphere. This behaviour is observed for all carried out experiments, and the mass increase is independent of the heating rate. This mild oxidation of DHA is based on its susceptibility of taking part in redox equilibria, in agreement with previously reported data [40], but as well as with the fact that when subjected to thermal stress or in the presence of ultraviolet radiation, the peroxide moiety can

Table 1 Thermoanalytical data obtained for DHA at the five selected heating rates

| β/°C min^{-1}	TG	Δm/%	DTG		HF	
	T_{onset}/°C		T_{onset}/°C	T_{peak}/°C	T_{onset}/°C	T_{peak}/°C
5	132	92.6	124	148; 160; 199	125	148; 159
7	132	91.9	124	150; 160; 207	125	150; 158
10	133	91.5	125	148; 160; 204	123	149; 158
12	134	90.6	125	149; 160; 198	124	149; 158
15	135	89.8	126	149; 160; 204	125	150; 158

form highly reactive radical species that can interact with dioxygen from the furnace atmosphere [9].

The observed thermal susceptibility of DHA is in agreement to data found in the literature, researchers mentioning several thermal degradation products obtained under thermal stress even in an inert dinitrogen atmosphere [41]. An apparently single-step decomposition that takes place in the 135–300 °C thermal range can be observed on the TG curves. During this interval, a mass loss of ≈ 91% was determined, the remaining residue calculated at the end of the analysis (500 °C) being ≈ 3%, indicating a significant mass loss suffered by DHA amid the applied thermal treatment. However, the determined DTG data revealed that during thermooxidation, three different processes can be correlated with peaks reached around 150, 160 and 200 °C.

that find correspondent two intense exothermic events visible on the HF curves around 150 and 160 °C. The melting process of pure DHA takes place according to the literature [8, 9] between 153 and 154 °C, but without a clear indication of what protocol was used for estimation of this interval, namely if a melting point apparatus or thermoanalytical data were used. According to our findings, as indicated by the HF curves, a clear endothermic solid–liquid phase transition event is not individualized, but instead an intense exothermic decomposition is observed, leading to the conclusion that the physical process of phase transition is accompanied by a chemical degradation. Later on, in the kinetic study section of this paper, the NPK results confirm this supposition. The decomposition process of DHA starts at relatively low temperatures ($T_{onset} \approx 135$ °C), this value being inferior to

Table 2 The selected kinetic methods employed to evaluate the thermal degradation of DHA

Method	Equation	Graphical representation	References
Fr	$\ln(\beta \frac{d\alpha}{dT}) = \ln[A \cdot f(\alpha)] - \frac{E_a}{R \cdot T}$	$\ln(\beta \frac{d\alpha}{dT})$ vs. $(1/T)$	[20]
FWO	$\ln \beta = \ln \frac{AE}{R \cdot g(\alpha)} - 5.331 - \frac{1.052 \cdot E_a}{R \cdot T}$	$\ln\beta$ vs. $(1/T)$	[21–23]
KAS	$\ln \frac{\beta}{T^2} = \ln \frac{A \cdot R}{E_a \cdot g(\alpha)} - \frac{E_a}{R \cdot T}$	$\ln(\beta/T^2)$ vs. $1/T$	[24, 25]
NPK	$\frac{d\alpha}{dT} = k(T) \cdot f(\alpha)$	3D	[26–31]
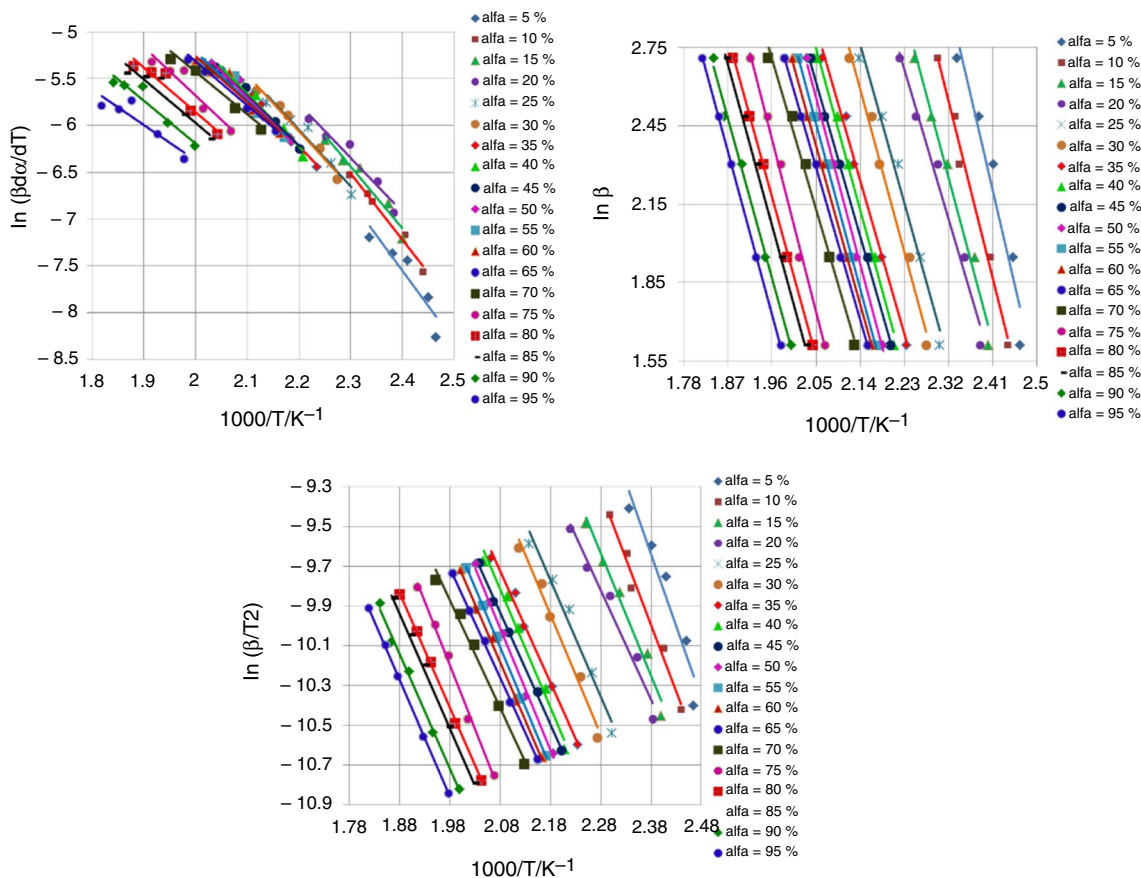
Fig. 4 Plotting of isoconversional methods for DHA: Fr (**a**), FWO (**b**) and KAS (**c**)

the reported temperatures associated with the melting process in previously published studies [8, 9]. However, the instability of DHA under thermal stress is in agreement with published data regarding the decomposition followed by complete destruction of the organic structure happening during high-temperature thermolysis [9, 41].

Kinetic study

As an important step in the investigation of stability of active pharmaceutical ingredients, kinetic analysis offers information about the decomposition mechanism and its dependence over thermal treatment regime that is applied to solid samples [35, 42, 43].

In order to complete the solid-state characterization of DHA, the kinetic triplet for the thermolysis of DHA was evaluated in dynamic dioxygen atmosphere, since, to our knowledge, no literature data were previously reported in the literature. As such, the non-isothermal ICTAC 2000 protocol was followed [34, 44–47] and three isoconversional methods (the differential Friedman (Fr) method and the Flynn–Wall–Ozawa (FWO) and Kissinger–Akahira–Sunose (KAS) integral methods) were used in order to determine, in the first step, the apparent activation energy values (E_a). Although neither the reaction order (n) nor the pre-exponential factor (A) is revealed using these methods, the isoconversional techniques provide estimations of the E_a values in relation to the conversion degree (α) without requiring the knowledge of exact form of the integral or differential conversion function. In order to complete the estimation of the parameters forming the kinetic triplet, the nonparametric kinetic method (NPK) was employed. The used mathematic models for each selected kinetic method are presented in Table 2.

Starting from the equations presented in Table 2 for each isoconversional method, the obtained data pairs were plotted and using the slopes determined for each straight line, the value of the activation energy was calculated according to the conversion degree (Fig. 4). The exact values obtained using each isoconversional method are presented in Table 3. The values collected for E_a were determined taking into consideration each value for the conversion degree found between the $5\% \leq \alpha \leq 95\%$ range while using a 5% variation step.

Studying the data presented in Table 3, it can be observed that the values obtained for the activation energy vary with the degree of conversion. This fact leads to the hypothesis that the process of decomposition of DHA is a complex one, consisting in more than one unitary process. This fact was also tentatively indicated by the analysis of the DTG curves and by the HF data, correlated with the melting behaviour reported in the literature. Regarding the observed E_a vs. α values, similar patterns were observed when the FWO and

Table 3 The E_a values obtained for each isoconversional method versus the conversion degree for DHA

α	Estimation of E_a (kJ mol^{-1}) by each kinetic method		
	FWO	KAS	Fr
0.05	64.0	60.4	63.1
0.1	59.5	55.6	58.9
0.15	55.5	51.2	54.6
0.2	50.3	45.7	48.1
0.25	53.3	48.6	49.8
0.3	54.8	50.1	49.9
0.35	51.6	46.6	46.6
0.4	54.2	49.2	46.8
0.45	52.0	46.9	44.4
0.5	56.0	51.0	46.2
0.55	55.2	50.1	43.4
0.6	53.7	48.5	41.2
0.65	51.4	46.1	39.2
0.7	50.6	45.0	37.7
0.75	58.5	53.2	43.2
0.8	54.0	48.3	39.7
0.85	54.1	48.3	38.9
0.9	53.9	48.0	38.1
0.95	54.8	48.9	31.7
$\bar{E}_a$ /kJ mol^{-1}	54.6 ± 0.8	49.6 ± 0.8	45.3 ± 1.8

KAS methods were employed, this fact being a predictable outcome, since the only difference between these two integral methods is represented by the approximation used for the conversion function in its integral form.

The variation of the results falls mostly in the $\pm 10\%$ limit around the mean value for both FWO and KAS methods, but presents an irregular pattern for the E_a values determined using the Fr method, an expected result considering the differential processing of the data by this method.

Because of these irregular patterns suggested by isoconversional methods, suggesting that a multistep decomposition occurs during thermolysis of DHA, the NPK method was further employed so as to process the kinetic data and to obtain the kinetic triplet without any approximations.

The NPK method has its bases on a single kinetic approximation, stating that the reaction rate (r) is a product of two separable functions (Eq. 1), where the rate constant k is temperature dependent and the differential conversion function f is α dependent:

$$r = \mathrm{d}\alpha(\mathrm{d}T)^{-1} = k(T)f(\alpha) \tag{1}$$

Using the experimental reaction rate values, a matrix expressed as a two-vector product (u_0 and v_0) can be formed. In this, each reaction rate is calculated according to Eq. 2:

$$r_{ij} = k(T_i)f(\alpha_j) \tag{2}$$

$$f(\alpha) = \alpha^m(1-\alpha)^n \tag{3}$$

The actual NPK method follows the next steps. First, the reaction rate surface is partitioned by intersecting the selected point for the matrix formation with two families of plans: one parallel with the temperature axis leading to the formation of isoconversional curves, and one parallel with the conversion degree axis generating isothermal curves. A 3D network is, as such, formed, and its intersection points represent the selected r_{ij}. Following this, the formed matrix is decomposed after the singular value decomposition algorithm (SVD) into a submatrix, separating the two factors that determine the reaction rate and making them independent from each other. In the last step, for each function, namely $k(T)$ and $f(\alpha)$, mathematical models must be assumed. Usually, for the temperature-dependent $k(T)$ function, the Arrhenius equation is selected, while for the conversion function, the Sestak–Berggren [48] equation is indicated (Eq. 3).

where m and n are specific parameters for each investigated process. Their significance is associated with physical transformations (when a $m \neq 0$ value is obtained) and/or chemical transformations (when a $n \neq 0$ value is obtained).

The kinetic analysis realized using the NPK method leads to the graphical representation of the most appropriate conversion functions, revealing the simulated and determined values for the normalized vectors u corresponding to the main and secondary decomposition processes (Fig. 5a) as well as a 3D visual representation of the experimental points together with the interpolation of the reaction rate as a continuous surface (Fig. 5 b).

The NPK obtained data for thermolysis of DHA are presented in Table 4. According to these, the decomposition of DHA during thermal stress is a consequence of two parallel steps, characterized by two sets of kinetic parameters (E_a,
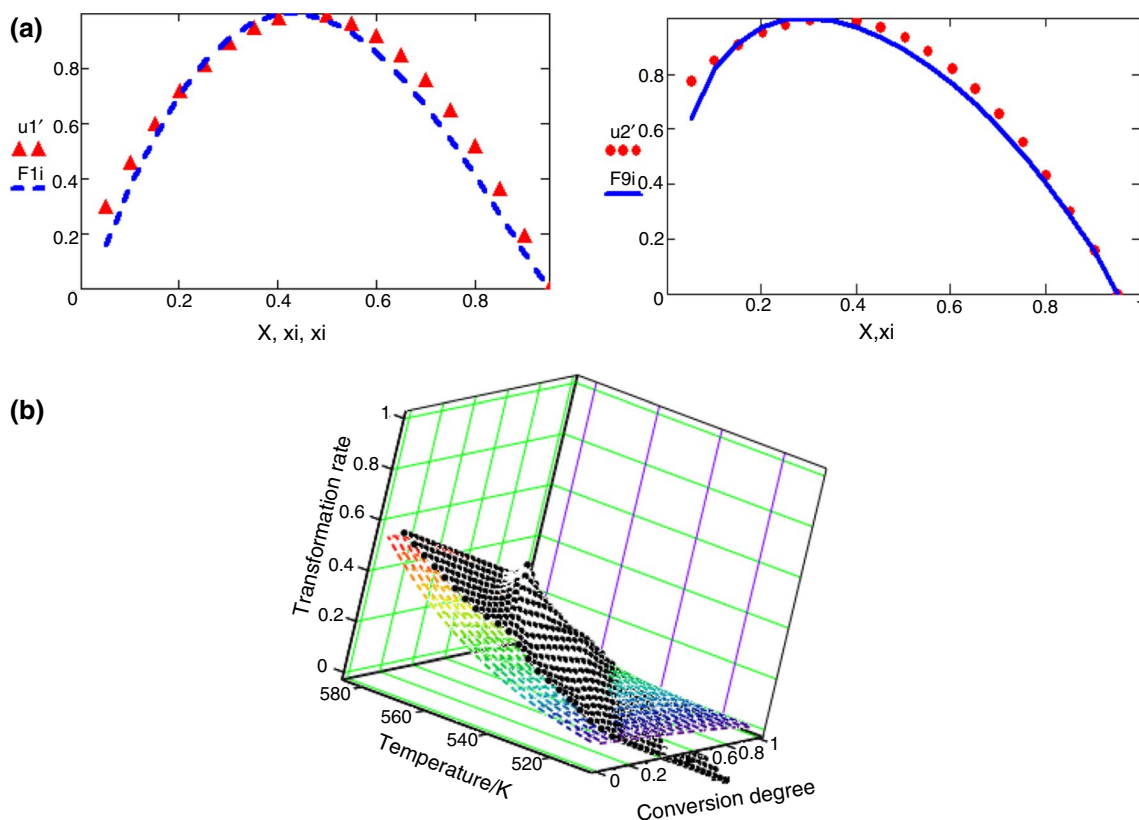
Fig. 5 Graphical representation for DHA of the conversion functions (**a**) and the 3D transformation rate surface (**b**) according to the NPK method

Table 4 The results obtained using the NPK method for DHA

Step	λ/ %	A/s^{-1}	E_a/kJ mol^{-1}	n	m	f(α)	R^2	$\bar{E}_a$ /kJ mol^{-1}
Main	69.8	1.96×10^6	54.4 ± 4.7	4/3	1	$\alpha (1-\alpha)^{4/3}$	0.990	58.0 ± 5.5
Secondary	30.2	9.78×10^5	66.2 ± 7.4	4/5	1	$\alpha (1-\alpha)^{4/5}$	0.993	

A, m and *n*), each process having a partial contribution to the global kinetic process, expressed as explained variance, λ. Both of these steps have a high contribution to the apparent mean activation energy value due to the fact that the values determined for the explained variance, λ, are approximately 70% and 30%, respectively. In the case of both steps, the DHA's complex decomposition mechanism suggested by the NPK data was proved to be determined by both chemical degradations (main step with $n = 4/3$ and secondary step with $n = 4/5$) and physical transformations (both main and secondary processes having $m = 1$). This last observation can be correlated with the information suggested by the analysis of thermoanalytical curves, where the melting process (which is a physical process) is accompanied by the chemical degradation of DHA.

Conclusions

In an effort to provide additional information regarding the physico-chemical profile of DHA, the present study reported an instrumental solid-state analysis of the first-line antimalarial and potential anticancer agent. After confirming the identity and purity of DHA using spectroscopic technique (ATR-FTIR analysis), thermoanalytical investigations were carried out in order to evaluate the stability and kinetic for oxidative thermolysis of DHA. The performed thermal analysis (TG/DTG/HF) revealed a relatively low stability for DHA when subjected to thermal stress, which is an important aspect to be considered during the currently used manufacturing processes, but also during the development of new solid dosage forms, that are currently performed by various research teams. The multiple step decomposition process observed in an oxidative atmosphere was revealed to take place simultaneously with the melting of DHA, as later on was confirmed by the use of NPK method.

In order to unveil the kinetic triplet that is associated with the thermooxidation of this drug, an in-depth analysis was performed. Since the two integral (FWO and KAS) and one differential (Fr) isoconversional methods employed revealed inconsistencies regarding the values of the apparent estimated E_a vs. α, the NPK method was used. As such, a two-step decomposition process was disclosed for DHA, both consisting in significant, albeit different, contributions to the mean apparent activation energy value. It was also revealed that both chemical degradations and physical transformations are involved in both processes determining the thermooxidation of the active pharmaceutical agent DHA.

References

1. Karunajeewa HA. Artemisinins: artemisinin, dihydroartemisinin, artemether and artesunate. In: Staines HM, Krishna S, editors. Treatment and prevention of Malaria. Basel: Springer; 2012. p. 157–90.
2. Njuguna NM, Ongarora DSB, Chibale K. Artemisinin derivatives: a patent review (2006–present). Expert Opin Ther Pat. 2012;22(10):1179–203.
3. Efferth T. Willmar Schwabe Award 2006: antiplasmodial and antitumor activity of artemisinin—from bench to bedside. Planta Med. 2007;73(4):299–309.
4. Ho WE, Peh HY, Chan TK, Wong WSF. Artemisinins: pharmacological actions beyond anti-malarial. Pharmacol Ther. 2014;142(1):126–39.
5. Tang W, Eisenbrand G. Chinese drugs of plant origin. chemistry, pharmacology, and use in traditional and modem medicine. 1st ed. Berlin: Springer; 1992.
6. Meshnick SR. Artemisinin: mechanisms of action, resistance and toxicity. Int J Parasitol. 2002;32(13):1655–60.
7. Cabri W, D'Acquarica I, Simone P, et al. Stereolability of dihydroartemisinin, an antimalarial drug: a comprehensive kinetic investigation. Part 2. J Org Chem. 2011;76(12):4831–40.
8. Haynes RK. From artemisinin to new artemisinin antimalarials: biosynthesis, extraction, old and new derivatives, stereochemistry and medicinal chemistry requirements. Curr Top Med Chem. 2006;6(5):509–37.
9. Jansen FH, Soomro SA. Chemical instability determines the biological action of the artemisinins. Curr Med Chem. 2007;4(30):3243–59.
10. Dhooghe L, Van Miert S, Jansen H, Vlietinck A, Pieters L. A new decomposition product of dihydroartemisinin. Planta Med. 2007;73(09):10–2.
11. Wang D, Li H, Gu J, Guo T, Yang S, Guo Z, Zhang X, Zhu W, Zhang J. Ternary system of dihydroartemisinin with hydroxypropyl-β-cyclodextrin and lecithin: simultaneous enhancement of drug solubility and stability in aqueous solutions. J Pharm Biomed Anal. 2013;83:141–8.
12. Binh TQ, Ilett KF, Batty KT, Davis TME, Hung NC, Powell SM, Thu LTA, Van Thien H, Phuöng HL, Phuong VDB. Oral bioavailability of dihydroartemisinin in Vietnamese volunteers and in patients with falciparum malaria. Br J Clin Pharmacol. 2001;51(6):541–6.
13. Batty KT, Ilett KF, Davis TME. Protein binding and α:β anomer ratio of dihydroartemisinin in vivo. Br J Clin Pharmacol. 2004;57(4):529–33.
14. Omwoyo WN, Melariri P, Gathirwa JW, Oloo F, Mahanga GM, Kalombo L, Ogutu B, Swai H. Development, characterization and antimalarial efficacy of dihydroartemisinin loaded solid lipid nanoparticles. Nanomed Nanotechnol Biol Med. 2016;12(3):801–9.
15. Righeschi C, Coronnello M, Mastrantoni A, Isacchi B, Bergonzi MC, Mini E, Bilia AR. Strategy to provide a useful solution to effective delivery of dihydroartemisinin: development, characterization and in vitro studies of liposomal formulations. Colloids Surf B Biointerfaces. 2014;116:121–7.
16. Li H, Li X, Shi X, Li Z, Sun Y. Effects of magnetic dihydroartemisinin nano-liposome in inhibiting the proliferation of head and neck squamous cell carcinomas. Phytomedicine. 2019;56(398):215–28.
17. Wang Z, Duan X, Lv Y, Zhao Y. Low density lipoprotein receptor (LDLR)-targeted lipid nanoparticles for the delivery of sorafenib and Dihydroartemisinin in liver cancers. Life Sci. 2019;239(July):117013.

18. Ansari MT, Iqbal I, Sunderland VB. Dihydroartemisinin-cyclo-dextrin complexation: solubility and stability. Arch Pharm Res. 2009;32(1):155–65.

19. Ansari MT, Imran M, Hassan SSU, Tariq I, Murtaza G. Solubility enhancement of dihydroartemisinin using mixture of hydroxypropyl-β-cyclodextrin and PEG-6000. Lat Am J Pharm. 2014;33(3):483–91.

20. Friedman HL. New methods for evaluating kinetic parameters from thermal analysis data. J Polym Sci Part B Polym Lett. 1969;7(1):41–6.

21. Flynn JH, Wall LA. A quick, direct method for the determination of activation energy from thermogravimetric data. J Polym Sci Part B Polym Lett. 1966;4(5):323–8.

22. Ozawa T. A New Method of Analyzing Thermogravimetric Data. Bull Chem Soc Jpn. 1965;38(11):1881–6.

23. Ozawa T. Kinetic analysis of derivative curves in thermal analysis. J Therm Anal. 1970;2(3):301–24.

24. Kissinger HE. Reaction Kinetics in Differential Thermal Analysis. Anal Chem. 1957;29(11):1702–6.

25. Akahira T, Sunose T. Research report, Trans joint convention of four electrical institutes. Chiba Inst Technol (Sci Technol). 1971;16:22–31.

26. Serra R, Sempere J, Nomen R. A new method for the kinetic study of thermoanalytical data: the non-parametric kinetics model. Thermochim Acta. 1998;316(1):37–45.

27. Serra R, Sempere J, Nomen R. The non-parametric kinetics. A new method for the kinetic study of thermoanalytical data. J Therm Anal. 1998;52:933–43.

28. Sempere J, Nomen R, Serra R. Progress in non-parametric kinetics. J Therm Anal Calorim. 1999;56(2):843–9.

29. Sempere J, Nomen R, Serra R, Soravilla J. The NPK method. Thermochim Acta. 2002;388(1–2):407–14.

30. Vlase T, Vlase G, Doca N, Bolcu C. Processing of non-isothermal TG data—comparative kinetic analysis with NPK method. J Therm Anal Calorim. 2005;80(1):59–64.

31. Vlase T, Vlase G, Birta N, Doca N. Comparative results of kinetic data obtained with different methods for complex decomposition steps. J Therm Anal Calorim. 2007;88(3):631–5.

32. Xiao D, Yang B, Zhao YL, Liao XL, Yang XM, Wang F, Chen YJ, Zhou RG. Inclusion complexes of dihydroartemisinin with cyclodextrin and its derivatives: characterization, solubilization and inclusion mode. J Incl Phenom Macrocycl Chem. 2014;79(3–4):349–56.

33. Circioban D, Ledeti A, Vlase G, Moaca A, Ledeti I, Farcas C, Vlase T, Dehelean C. Thermal degradation, kinetic analysis and evaluation of biological activity on human melanoma for artemisinin. J Therm Anal Calorim. 2018;134(1):741–8.

34. Vyazovkin S, Chrissafis K, Di Lorenzo ML, Koga N, Pijolat M, Roduit B, Sbirrazzuoli N, Suñol JJ. ICTAC Kinetics Committee recommendations for collecting experimental thermal analysis data for kinetic computations. Thermochim Acta. 2014;590:1–23.

35. Ledeti A, Vlase G, Vlase T, Circioban D, Dehelean C, Ledeti I. Kinetic study for solid-state degradation of mental disorder therapeutic agents. J Therm Anal Calorim. 2018;131(1):155–65.

36. Ledeti I, Ledeti A, Vlase G, Vlase T, Matusz P, Bercean V, Suta LM, Piciu D. Thermal stability of synthetic thyroid hormone l-thyroxine and l-thyroxine sodium salt hydrate both pure and in pharmaceutical formulations. J Pharm Biomed Anal. 2016;125:33–40.

37. Ledeti I, Vlase G, Vlase T, Bercean V, Fulias A. Kinetic of solid-state degradation of transitional coordinative compounds containing functionalized 1,2,4-triazolic ligand. J Therm Anal Calorim. 2015;121(3):1049–57.

38. Suta L, Vlase G, Vlase T, et al. Solid State Stability of Cholesterol. Preliminary kinetic analysis. Rev Chim. 2016;67(1):113–5.

39. Ledeti I, Pusztai AM, Muresan CM, et al. Study of solid-state degradation of prochlorperazine and promethazine. J Therm Anal Calorim. 2018;134(1):731–40.

40. Cabello CM, Lamore SD, Bair WB, Qiao S, Azimian S, Lesson JL, Wondrak GT. The redox antimalarial dihydroartemisinin targets human metastatic melanoma cells but not primary melanocytes with induction of NOXA-dependent apoptosis. Invest New Drugs. 2012;30(4):1289–301.

41. Haynes RK, Chan HW, Lung CM, Ng AC, Wong HN, Shek LY, Williams ID, Cartwright A, Gomes MF. Artesunate and dihydroartemisinin (DHA): unusual decomposition products formed under mild conditions and comments on the fitness of DHA as An Antimalarial Drug. ChemMedChem. 2007;2(10):1448–63.

42. Ledeti A, Olariu T, Caunii A, Vlase G, Circioban D, Baul B, Ledeti I, Vlase T, Murariu M. Evaluation of thermal stability and kinetic of degradation for levodopa in non-isothermal conditions. J Therm Anal Calorim. 2018;131(2):1881–8.

43. Circioban D, Ledeţi I, Vlase G, Ledeţi A, Axente C, Vlase T, Dehelean C. Kinetics of heterogeneous-induced degradation for artesunate and artemether. J Therm Anal Calorim. 2018;134(1):749–56.

44. Dickinson CF, Heal GR. A review of the ICTAC kinetics project, 2000. Thermochim Acta. 2009;494(1–2):15–25.

45. Vyazovkin S. Computational aspects of kinetic analysis. Thermochim Acta. 2000;355(1–2):155–63.

46. Brown ME, Maciejewski M, Vyazovkin S, et al. Computational aspects of kinetic analysis. Thermochim Acta. 2000;355(1–2):125–43.

47. Vyazovkin S, Burnham AK, Criado JM, Pérez-Maqueda LA, Popescu C, Sbirrazzuoli N. ICTAC Kinetics Committee recommendations for performing kinetic computations on thermal analysis data. Thermochim Acta. 2011;520(1–2):1–19.

48. Sestak J, Berggren G. Study of the kinetics of the mechanism of solid-state reactions at increasing temperatures. Thermochim Acta. 1971;3(1):1–12.